KAWASAKI STEEL TECHNICAL REPORT
No.4 (December 1981)
Special Issue on Steel Pipe

Steel Sheet Deformation Behavior and Forming Load Determination in the 26-inch Cage Forming ERW Pipe Mill

Eiichi Yokoyama, Takaaki Toyooka, Akio Ejima, Yuzo Yoshimoto, Takao Kawate, Kazuyoshi Kuwata

Synopsis :
Behavior of steel sheet deformation as expressed in strain history, projection trace and forming flowers, and methods of determining forming load as fin pass rolls and squeeze rolls have been investigated in the 26 in. cage forming ERW pipe mill. For the longitudinal strain of the sheet edge, only a gentle deformation is observed in the cage forming zone, while a considerably rapid deformation consisting mainly of tension and including compression is noticed at the time when the sheet passes through each fin pass roll. The local increase in wall thickness around the sheet edge is caused mainly by No.1 fin pass roll forming. On the contrary, almost uniform compressive deformation is conducted by No.2 fin pass roll forming. The forming load, which depends strongly on the strength and wall thickness of sheet, can be expressed by the summation of forces which are necessary for the circumferential reduction and the bending of sheet.

The body can be viewed from the next page.

Steel Sheet Deformation Behavior and Forming Load Determination in the 26-inch Cage Forming ERW Pipe Mill*

Eiichi YOKOYAMA** Takaaki TOYOOKA** Akio EJIMA**
Yuzo YOSHIMOTO*** Takao KAWATE*** Kazuyoshi KUWATA***

Behavior of steel sheet deformation as expressed in strain history, projection trace and forming flowers, and methods of determining forming load at fin pass rolls and squeeze rolls have been investigated in the 26 in. cage forming ERW pipe mill. For the longitudinal strain of the sheet edge, only a gentle deformation is observed in the cage forming zone, while a considerably rapid deformation consisting mainly of tension and including compression is noticed at the time when the sheet passes through each fin pass roll. The local increase in wall thickness around the sheet edge is caused mainly by No. 1 fin pass roll forming. On the contrary, almost uniform compressive deformation is conducted by No. 2 fin pass roll forming. The forming load, which depends strongly on the strength and wall thickness of sheet, can be expressed by the summation of forces which are necessary for the circumferential reduction and the bending of sheet.

1 Introduction

While the grooved roll forming method has prevailed so far for manufacturing medium diameter ERW pipe, the cage roll forming method has recently been reconfirmed as effective following the latest trend in medium diameter ERW pipe toward higher strength and larger diameters. With the 26 in. cage forming ERW pipe mill at the Chita works, high grade line pipe products of various sizes including fairly thin and thick wall thickness have mainly been manufactured since October 1978.

This mill[1-3] is characterized by the feature that it is equipped with several dozen pairs of cage rolls arranged to provide a bending process by applying the downhill forming prior to the fin pass forming process. This cage forming mill can reduce so-called "edge stretch" because of a more natural and less restrained forming as compared with the conventional grooved roll forming, so that it makes possible to increase the productivity and the variety of products. On the other hand, for improving the weld quality of ERW pipe, the forming condition from breakdown roll, through fin pass roll to squeeze roll is of great importance along with the optimum welding condition[4-7]. Especially in the case of thin wall thickness and large diameter pipe, establishment of the optimum forming condition is essential to prevent weld defects due to edge wave.

The selection and control of the forming condition, however, is not always satisfactory at the present time because it is sometimes left to the technical experience and perception based on a macroscopic variation in size and shape at the operation sites. The main reason for this situation is considered to be that, unlike press forming, theoretical analysis is very difficult for continuous roll forming because every part of a steel sheet is continuously subjected to three dimensional complex deformation, and the deformation behavior has not yet been resolved in terms of microscopic analysis.

To obtain fundamental knowledge on cage roll forming in this 26 in. ERW pipe mill, the following investigations have been made.

(1) Behavior of steel sheet deformation during the forming process.
(2) Determination of forming load at fin pass rolls and at squeeze rolls.

2 Experimental Procedure

2.1 Determination of Strain History

The layout of the 26 in. cage forming ERW pipe mill is shown in **Fig. 1**. It is desirable to measure the continuous strain of steel sheet from the downhill start before pre-forming roll to squeeze roll. However,

* Originally published in *Kawasaki Steel Giho*, 13 (1981) 1, pp. 80–92
** Research Laboratories
*** Chita Works

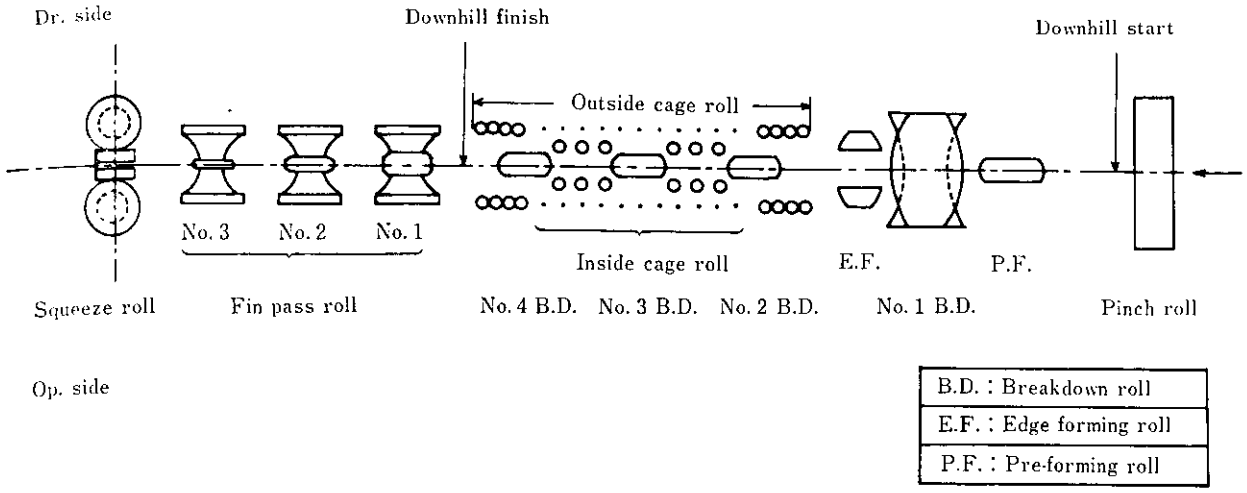

Fig. 1 Layout of 26 inch cage forming ERW mill

in order to prevent strain gage damage due to contact between steel sheet and each roll, the relative surface strain was measured in two separate sections, one from the pinch roll to the edge forming roll and the other from the edge forming roll to the squeeze roll.

Strain gages, KFC type of Kyowa Electric Instruments Co., Ltd., (gage size: 10 mmℓ × 3 mm$w$, base size: 16 mmℓ × 5 mm$w$) were stuck on the edge, at the center of the transverse direction and at the lateral face center of the sheet material as shown in **Fig. 2**. As for the center, measurement was made at a point slightly towards the operator side to avoid contact of the sheet with Nos. 2 to 4 breakdown rolls. On the lateral face center, strain gages were stuck close to the neutral axis of bending (approximately the center of the wall thickness direction) to estimate longitudinal membrane strain at the edge, on the assumption that the sum of the variations in gage resistance due to the bending strain was zero.

Table 1 shows chemical composition and mechanical properties of the hot rolled sheet (pipe size: 24 in. ϕ × 6.35 mm$t$, grade: API 5LX X60), and **Table 2** shows forming conditions in each stand-to-stand using the circumferential length of the sheet.

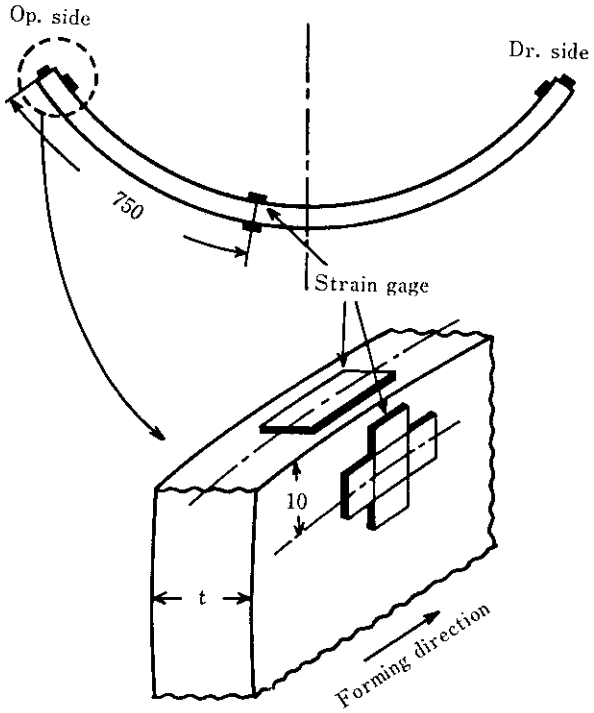

Fig. 2 Strain gage positions on the surface of sheet material

Table 1 Chemical composition and mechanical properties of hot rolled sheet

Grade	Pipe size	Chemical composition (wt%)								Mechanical properties		
		C	Si	Mn	P	S	Al	Nb	V	Y.S.* (kgf/mm²)	T.S. (kgf/mm²)	El. (%)
API 5LX X60	24 in. ϕ × 6.35 mm	0.07	0.21	1.09	0.018	0.003	0.026	0.027	0.031	54.7	59.8	33.2

(* : At 0.5% total strain)
Y.S. : Yield strength, T.S. : Tensile strength, El. : Elongation

Table 2 Forming conditions on the circumferential length of sheet along the outside surface

Measured positions		Circumferential length (mm)	Reduction (%)
P.F.	Entry side	1 927.3	−0.89
No.1 F.P.	Entry side	1 944.5	0.93
	Exit side	1 926.5	0.18
No.2 F.P.	Exit side	1 923.0	≒ 0
No.3 F.P.	Exit side	1 923.1	
S.Q.	Exit side	1 922.0	

P.F.: Pre-forming roll, F.P.: Fin pass roll
S.Q.: Squeeze roll

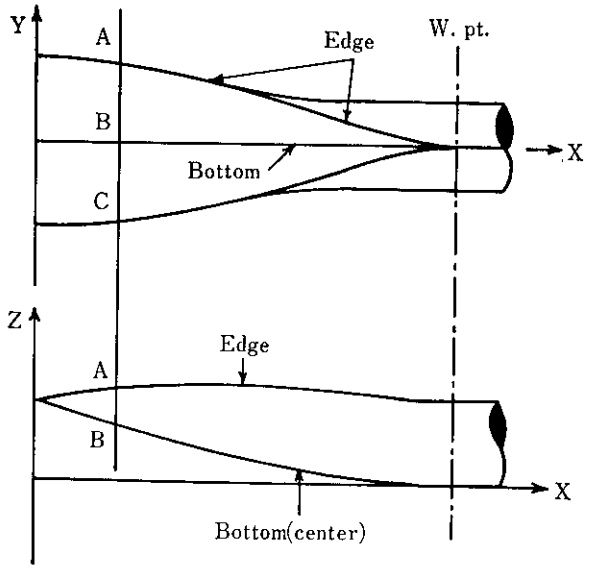

Fig. 3 Plan and side views of sheet deformation in pipe forming process

2.2 Measurement of Projection Traces

During the bending deformation as shown in **Fig. 3**, in order to clarify projection trace and forming flowers at the edge and center, distance between A and B and height from the base line at each position along A-B-C line on the sheet were measured.

2.3 Determination of Forming Loads

Strain gage positions on the fin pass and squeeze roll stands are shown in **Figs. 4** and **5**, respectively. Strain gage of the same kind as mentioned above was stuck at two to three positions on roll-supporting shafts, one each on the work side and the drive side, respectively, to measure forming loads during the manufacture of pipes of various sizes and grades. Values of strain or load mentioned later are those on either the work or the drive side, or the mean of both.

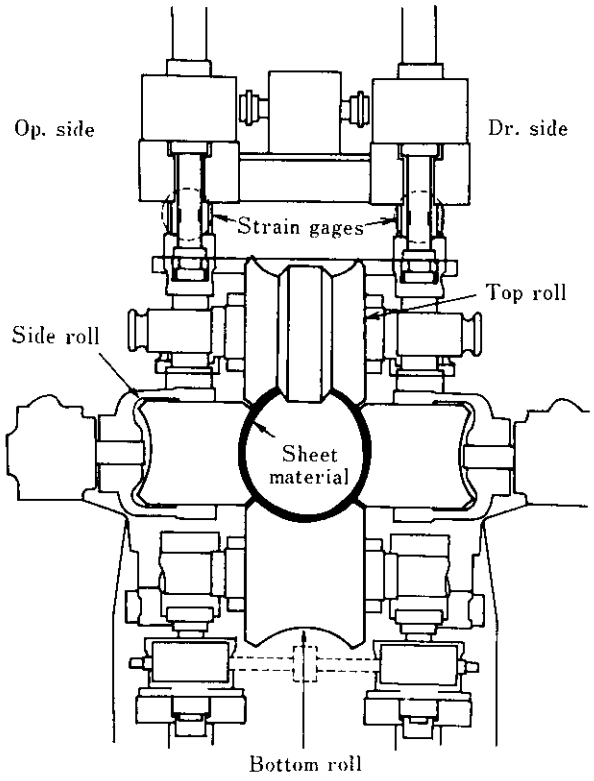

Fig. 4 Strain gage positions for measuring forming load in No. 1 fin pass top roll

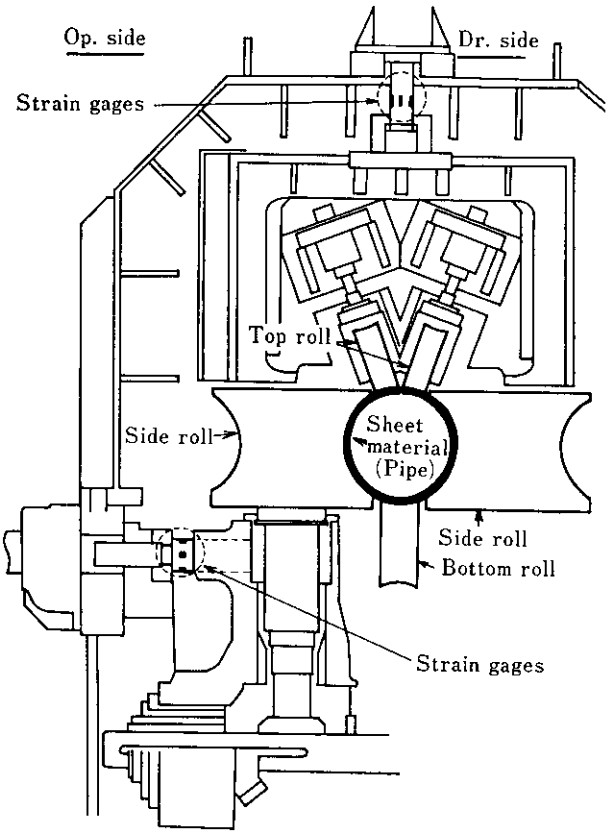

Fig. 5 Strain gage positions for measuring forming load in squeeze side and top rolls

3 Experimental Results

3.1 Strain during Pipe Forming

3.1.1 From the pinch roll to edge forming roll

Fig. 6 shows the longitudinal surface strain e_x and circumferential surface strain e_y at the inside edge and center. In the longitudinal direction at the edge, tensile strain shows a gentle increase making two peaks of about 0.3 to 0.4% at No. 5 dish roll on the exit side of the pre-forming roll and at No. 1 breakdown roll. After passing through No. 1 breakdown roll, a tensile strain of about 0.2% appears again, followed by some compressive deformation and then also by a rapid tensile strain of about 0.6% while going through the edge forming roll.

Such complex transition in strain corresponds well to the forming behavior of steel sheet in entering No. 1 fin pass roll mentioned later, and is considered to be caused by bending and unbending deformation due to fitting of the sheet to rolls.

Regarding the circumferential strain at the edge, a peak appears on the compression side corresponding to the transition in the longitudinal strain, but it is small enough to remain within the elastic region because the edge is not subjected to bending before the edge forming roll.

As for strain at the center, hardly any variation can be observed in the longitudinal direction and a gradual increase in compressive strain is produced by the slight but continuous bending in the circumferential direction.

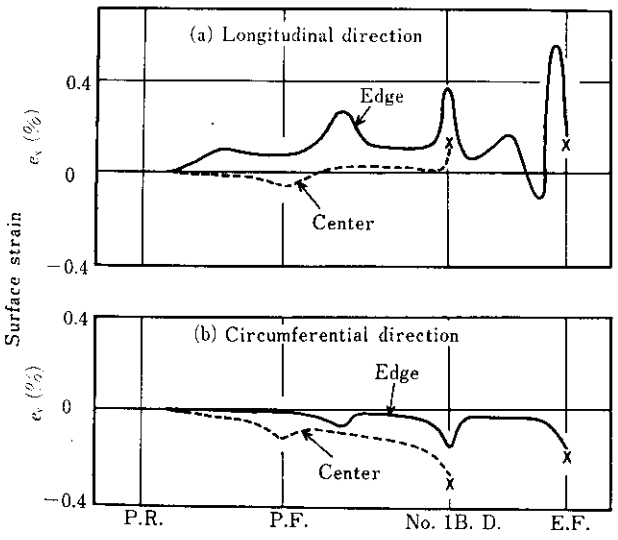

Fig. 6 Surface strain from pre-forming to edge forming

3.1.2 From edge forming roll to squeeze roll

The longitudinal strain is shown in **Fig. 7. Photo. 1** shows the near-edge forming condition in the cage zone, and **Photo. 2**, that during the entry to No. 1 fin pass roll. In the cage zone, little variation is observed in the longitudinal strain both at the edge and center. While, at the edge, a slight tensile deformation appears first and slowly shifts to compressive

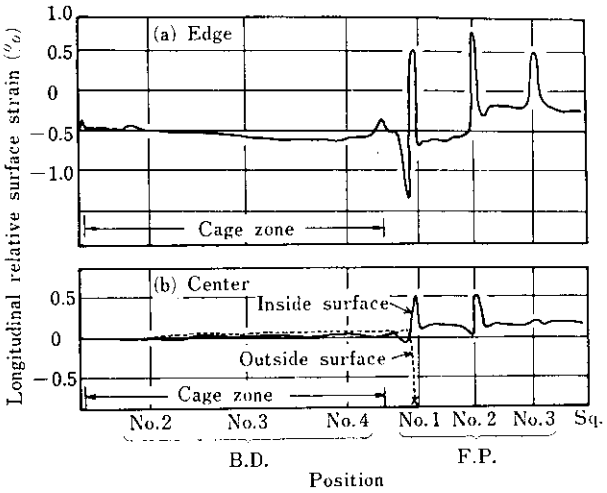

Fig. 7 Longitudinal surface strain in cage and fin pass forming

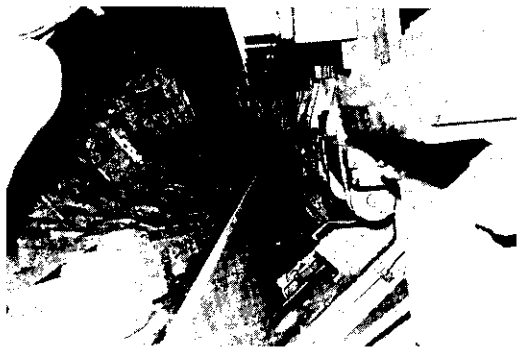

Photo. 1 Sheet edge forming in the cage zone

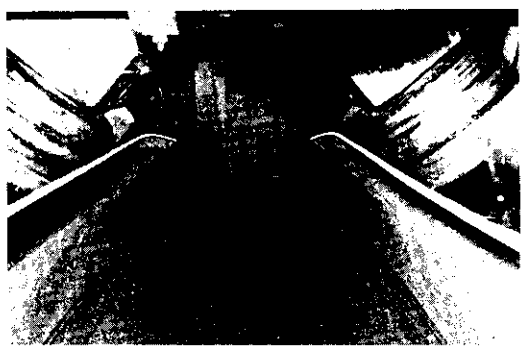

Photo. 2 Sheet edge forming at the entry to No. 1 fin pass roll

deformation, at the center only a slight and gentle increase in tensile strain is observed.

When the forming has advanced to the region ranging from the point where the sheet is released from the restraints of the last cage roll to its entrance into the No. 1 fin pass roll, it is noticed that a fairly large compressive deformation occurs in the longitudinal direction at the edge following a slight tensile deformation (see **Photo. 2**). Furthermore, a rapid tensile-compressive deformation is also noticed before and after passing through each fin pass roll.

Such a sharp variation of strain at the entrance into the roll was discussed in several reports on deformation of trapezoidal channel sections[8,9], circular arc sections[10], and V-type sections[11], and is understood to be caused by an overlapping of the forming factors as follows:

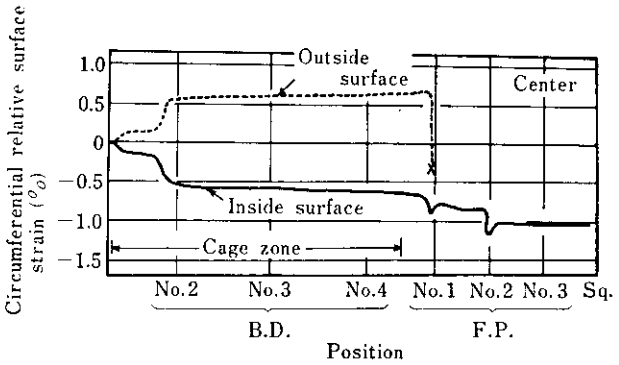

Fig. 8 Circumferential surface strain in cage and fin pass forming

(1) Bending and unbending deformation of steel sheet caused by its fitting to the roll.
(2) Compressive and tensile deformation in the longitudinal direction caused by space trace difference along the whole length of the sheet (e.g. edge and center).
(3) Deformation due to differences in distribution of force generated by directional change caused by movement of the sheet.

As mentioned above, the fin pass roll plays an exceptionally important role in correcting any sharp compressive deformation at the edge and preventing edge buckling phenomenon.

Fig. 8 shows the circumferential surface strain at the center. In the cage zone the compressive strain of the inside surface and the tensile strain of the outside surface increase gently after showing a sharp increase in the vicinity of No. 2 breakdown roll, and then the steel sheet is still subjected to a compressive deformation on each fin pass roll corresponding to bending and reducing condition.

3.2 Shape Change in Pipe Forming Process

Fig. 9 indicates projection traces (projection width and projection height) at the edge and center in the forming process prior to the entrance to No.1 fin pass roll. The bottom line shows a fall equivalent to the downhill height 0.8 × O.D. (Outside diameter), whereas the edge line rises gradually up to the middle region between Nos. 2 and 3 breakdown rolls in the

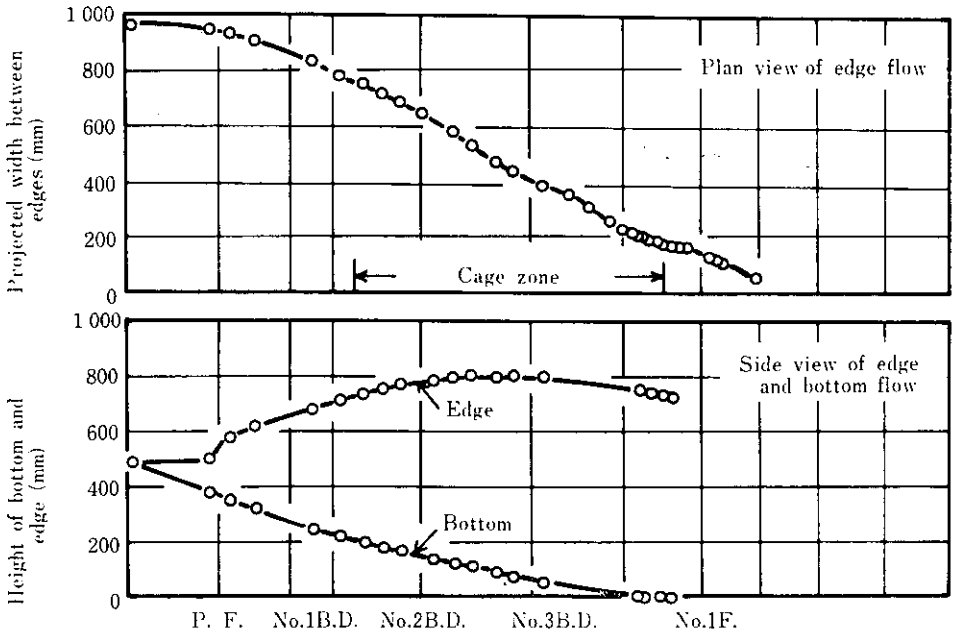

Fig. 9 Edge and center traces in pipe forming process

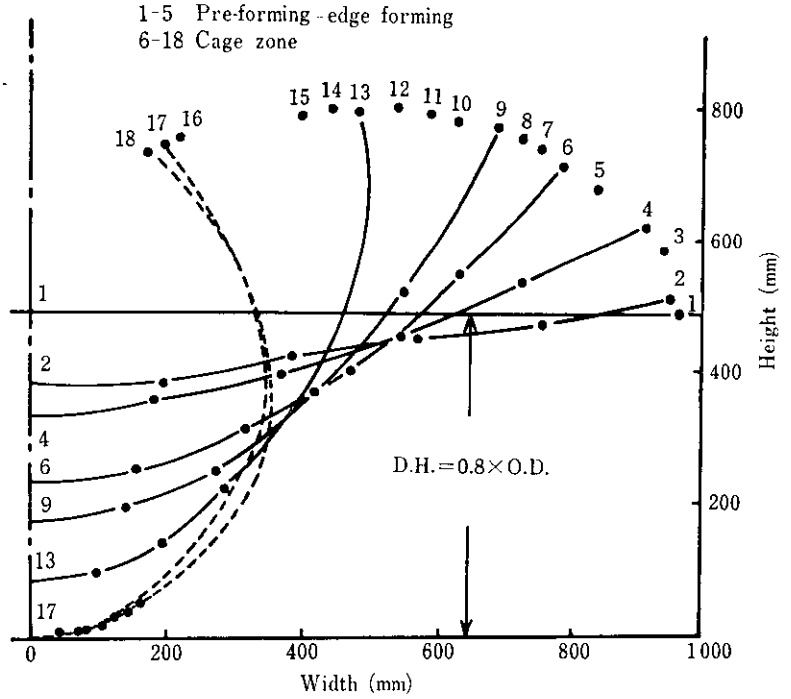

Fig. 10 Forming flower in the case of 0.8 × O.D. downhill height

cage zone ($\Delta H_{max} \cong 0.5 \times$ O.D.), and then gradually falls to shift into fin pass roll forming. **Fig. 10** shows the shape change of the forming sections (flower) measured at several longitudinal positions.

3.3 Measured Values of Forming Load

Fig. 11 shows the relation between forming load and $\sigma_y \cdot t$ (σ_y: yield strength of sheet, t: wall thickness) in No. 1 fin pass top roll, squeeze side roll and squeeze top roll. The forming load tends to increase with an increase of $\sigma_y \cdot t$, but considerable variation is observed because, as mentioned later, influences of fin pass reducing amount (Δl_F) and squeeze upset amount (Δl_s) on forming load are large.

4 Consideration

4.1 Cage Roll Forming

Various experiments and investigations[12-20] have been reported on downhill forming, which has been recommended to reduce trace differences between edge and center, and to prevent edge buckling phenomenon in the pipe forming process. Various values have also been reported as optimum downhill height because they vary with roll caliber, inter-roll stand distance and the number of rolls of the forming mill[13,14,17,18]. An excessive downhill forming is generally considered to produce a reverse effect by promoting edge buckling.

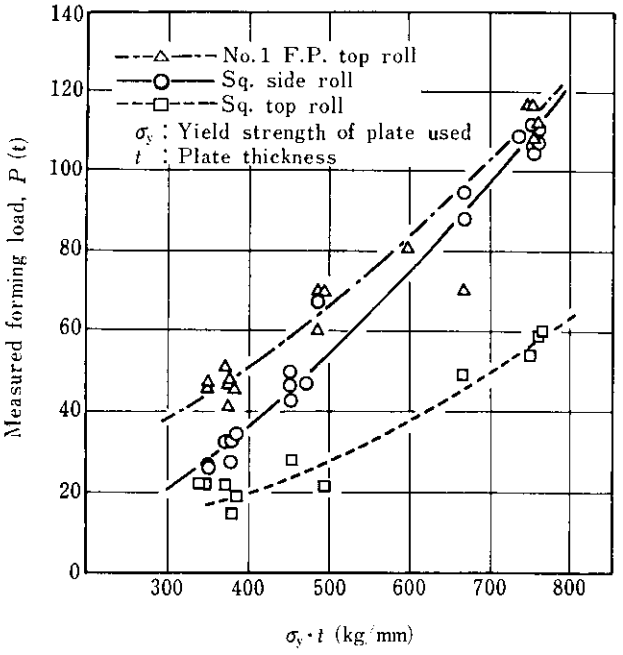

Fig. 11 Relation between forming load and $\sigma_y \cdot t$

Fig. 12 represents the longitudinal relative membrane strain at the edge and center in the cage roll forming region. Compressive strain increases gradually in the longitudinal direction at the edge, probably indicating that edge stretch is extremely restrained by the external forces owing to the number of cage rolls

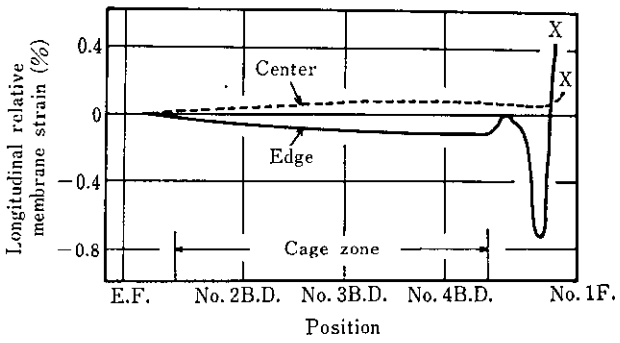

Fig. 12 Longitudinal relative membrane strain in cage forming process

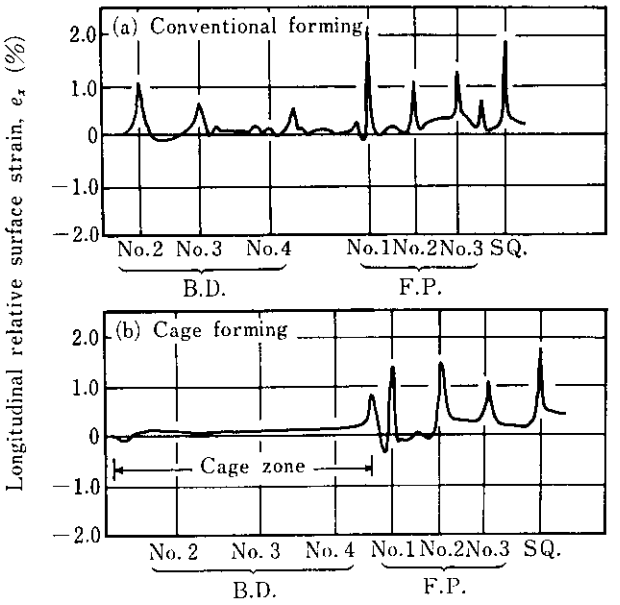

Fig. 13 Comparison of longitudinal surface strain at the sheet edge between conventional and cage forming processes (18 in. ϕ × 7.92 mm, X-52)

along with the effects of downhill forming because the stretch is absorbed to produce compressive strain.

In the longitudinal direction at the center, tensile strain gradually increases contrary to the case at the edge, suggesting the same effect as the center stretching method (a method to stretch the center of a sheet to reduce the difference in relative strain between edge and center) proposed by Baba[15], Namatame[16] et al.

Fig. 13 shows a comparison of the longitudinal relative strains in forming 18 in. ϕ × 7.92 mm$t$ (X-52) pipe between the conventional grooved roll mill (Mckay 20 in. mill) and this cage roll mill (IHI-Yoder 26 in. mill).

In the conventional breakdown roll forming, a rapid tensile-compressive deformation is observed before and after passing through each breakdown roll, suggesting an increases in edge stretch; whereas in the cage roll forming only a slight strain change appears, suggesting the effectiveness of this process.

It should be noticed, however, that in the cage roll forming the edge is subjected to a slight tensile deformation and then to a fairly large compressive deformation in the region ranging from the point where the sheet is released from the restraints of the last cage roll to its entrance into the No. 1 fin pass roll, as described above. A similar phenomenon is observed at the entry side of the edge forming roll. This indicates, as reported by Nakajima, Mizutani et al.[20], that although the cage forming is effective in respect of shifting edge stretch into compressive strain, edge buckling may possibly occur if the compressive stress state exceeds the buckling limit, thus making it essential to appropriately control the compressive deformation state. (In the case of this cage roll forming process, a strong bending is added around the edge by the edge forming roll, aiming at increasing the rigidity to prevent edge buckling).

4.2 Fin Pass Roll Forming

In the fin pass forming, an appropriate setting up and selection of roll alignment and reduction value are very important to prevent edge buckling and to obtain stable V shape and edge lateral face in the squeeze roll welding process. However, regarding the forming behavior, very few research has been reported and much remains unknown because of complex stress conditions subjected to sheet pipe in the fin pass forming region and difficulties in the measuring and analyzing procedures. So consideration has been made based on the data on strain history obtained in this experiment.

Fig. 14 shows the schematic diagram for the shape and strain of sheet edge during the fin pass rolling. The longitudinal bending strain along the throat radius R (= 300 mm) of the fin pass top roll is calculated at $\epsilon_{Xb} = t/(2R + t) = 1.05\%$ (t = 6.35 mm) which is very close to the measured value $\epsilon_X \fallingdotseq 1.10\%$ (see **Fig. 7**). This proves that the sharp tensile – compressive deformation produced at the entry to the fin pass roll is almost exclusively caused by the occurrence of bending and unbending strain due to fitting of the sheet to the throat of the fin pass top roll, and is supplemented by a slight, additional membrane strain due to fin pass reduction.

As for transition in the transverse surface strain at the center (see **Fig. 8**), about 0.12% and about 0.23% of reduction deformation are added before and after Nos. 1 and 2 fin pass rolls, respectively. On the other hand, compared with circumferential reduction of 0.93% for No. 1F and 0.18% for No. 2F, reduction in terms of the circumferential surface strain at the

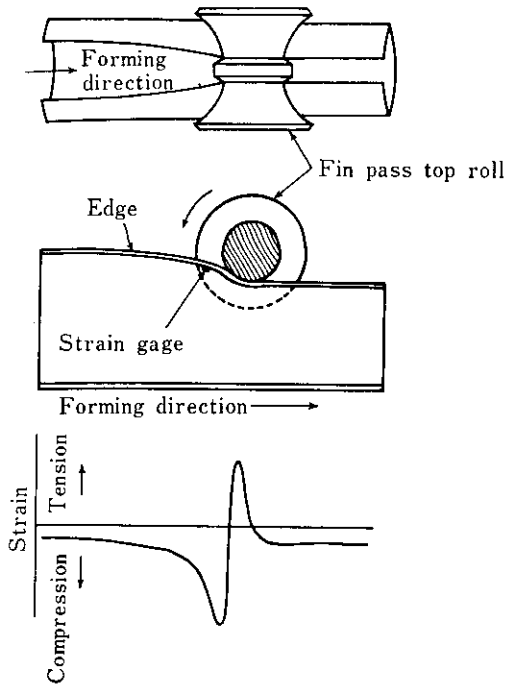

Fig. 14 Shape and strain of the sheet edge during fin pass rolling

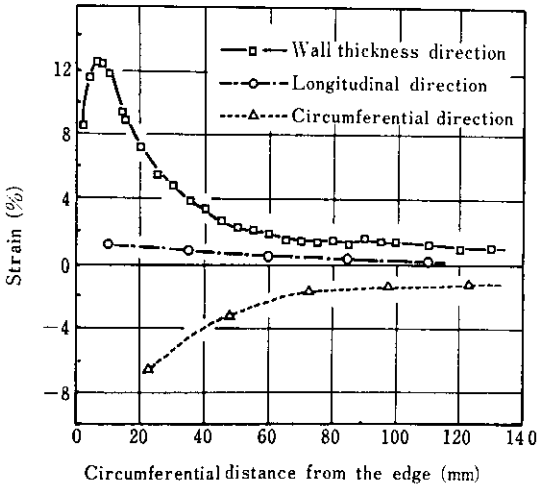

Fig. 15 Strain distribution in triaxial directions in the vicinity of sheet edge caused by fin pass roll forming

center is larger in the No. 2 fin pass forming. On the contrary, the circumferential reduction is apparently much larger in No. 1 fin pass forming. (In this experiment the reduction given in No. 3 fin pass roll is very small.)

The bending strain difference between No. 1 and No. 2 fin pass rolls, $\Delta\epsilon_{yb}$, can be estimated at 0.05% from the groove radius of each fin pass bottom roll, and the difference of the measured internal surface strain before and after No. 2 fin pass roll is 0.23%, which consists of bending and membrane strain. Therefore, the compressive membrane strain produced by No. 2 fin pass roll, can be calculated at 0.18%, which corresponds to the difference between 0.23% and 0.05%, and shows a good agreement with the reduction value obtained from the circumferential outside surface length (0.18%).

Fig. 15 shows the strain distribution in triaxial directions (longitudinal: ϵ_ℓ, circumferential: ϵ_c, wall thickness: ϵ_t) in the vicinity of the sheet edge caused by fin pass roll forming; the distribution is determined by the scribed circle method and from wall thickness variations. Among these three strains there is an approximate constant volume relationship $\epsilon_\ell + \epsilon_c + \epsilon_t = 0$). Although each strain varies according to the various restrained conditions, rolling conditions and quality and shape of sheet, predominant increase of wall thickness is observed particularly around the sheet edge.

The tensile strain due to increase of wall thickness is greatest at about 10 mm portions from the sheet edge in the circumferential direction and is not so great around the lateral face of the sheet edge; this is assumed to be caused by the shear drop due to side trimming and the restraint at fin face.

The above results show the fact that the reducing deformation at No. 1 fin pass roll is virtually concentrated around the edge to increase wall thickness, whereas an almost uniform compressive deformation is caused by fairly uniform restraint in the circumferential direction at No. 2 fin pass roll where the sheet is formed into nearly a true circular shape, becoming fitted to the roll groove shape. This agrees well with an experimental finding by Kiuchi et al.[21] to the effect that the wall thickness tends to increase locally around the sheet edge especially in the first fin pass roll with a larger width and angle of fin because the force acting on the edge is greater in the circumferential direction than in the radius direction. Therefore, increasing the wall thickness around the edge by giving a high forming reduction at No. 1 fin pass roll is effective in preventing edge buckling, because any induced edge buckling is absorbed in the wall thickness direction and increases the buckling resistance. This agrees well with the experimental results on a cage roll model mill by Onoda et al.[22] and with the report by Baba[15].

4.3 Forming Load

When a rolling force works on pipe in the circumferential direction such as in fin pass forming or squeeze roll forming, the forming load is not only affected complicatedly by roll arrangement, roll groove, roll diameter and the circular arc shape of

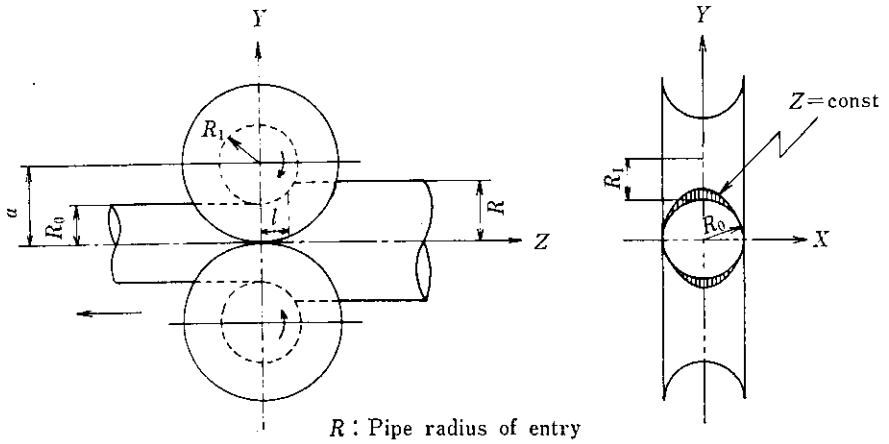

Fig. 16 Schematic diagram of contact area on the outside surface of pipe reduced by two rolls[24]

steel sheet, but it also behaves differently depending on a steady or unsteady state in tandem forming[23].

Therefore, the explicit analysis of forming load has been said to be considerably difficult. In the simplified two-roll type true circular roll as shown in **Fig. 16**, Nakajima, Mizutani, et al.[12,24] introduced eq. **(1)**, taking l as the distance in the longitudinal direction within the region where compressive force acts on the pipe in the circumferential direction. In addition, at the starting line in this region, the circumferential length of the sheet corresponds to the circumferential length of the roll section parallel to the roll axis direction.

$$l = 2R_0\sqrt{(a/R_0 - 1)r} \quad \cdots\cdots\cdots\cdots (1)$$

R_0: Pipe radius of exit
a: Roll flange radius
r: Fin pass reduction

Eq. **(1)** can be transformed to eq. **(1)'**

$$l = \sqrt{2R_1/\pi}\cdot\sqrt{\Delta l_C} \quad \cdots\cdots\cdots\cdots (1)'$$

R_1: Roll bottom radius
Δl_C: Reduction at fin pass roll or squeeze roll

Forming force per unit length is expressed by

$$F = 2\sigma_y \cdot t \cdot \sin\theta^{25} \quad \cdots\cdots\cdots\cdots (2)$$

2θ: roll angle

Compressive forming load on roll $P = l \cdot F$ is transformed to eq. **(3)** from eqs. **(1)** and **(2)**

$$P = 2\sigma_y \cdot t \cdot \sin\theta \cdot \sqrt{2R_1/\pi} \cdot \sqrt{\Delta l_C} \quad \cdots\cdots (3)$$

(It is assumed here that eq. **(1)'** is approximately true also for fin pass and squeeze roll with two rolls or more.)

It is empirically known that the actual forming load does not become 0 even when $\Delta l_C = 0$, because the pipe shape of entry is never truly circular, requiring bending forming force. Some experimental analyses[26-29] have been made on the bending load (P_B) of sheet. Nakajima and Mizutani[28,29] et al. confirmed by laboratory experiment that P_B in breakdown roll is propotional to the square of wall thickness, hence the following equation.

$$P_B = \alpha \cdot \sigma_y \cdot t^2 \quad \cdots\cdots\cdots\cdots (4)$$

In the eq. **(4)**, α is a constant term, depending on roll shape, bending shape and quality of the sheet, generally termed the load correction coefficient. Consequently, the actual forming load can be expressed as the sum of forces necessary for the circumferential reduction and the bending of sheet by eq. **(5)** deduced from eqs. **(3)** and **(4)**

$$P = 2\sigma_y \cdot t \cdot \sin\theta\sqrt{2R_1/\pi} \cdot \sqrt{\Delta l_C} + \alpha \cdot \sigma_y \cdot t^2 \quad \cdots\cdots (5)$$

Using Δl_F (circumferential reducing amount in No. 1 fin pass roll) and Δl_S (upset amount in squeeze roll) for Δl_C the relationship between actual load and parameter, $t \cdot \sigma_y\sqrt{\Delta l_C}$, is shown for No. 1 fin pass top roll and squeeze side roll in **Figs. 17** and **18**, respectively. A close linearity was observed between

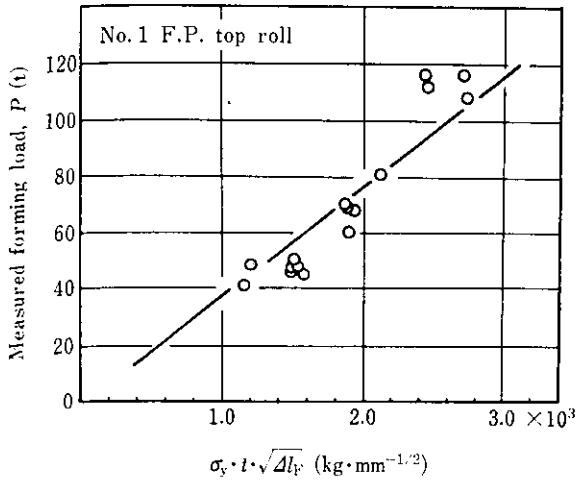

Fig. 17 Relation between forming load and a parameter, $\sigma_y t \cdot \sqrt{\Delta l_F}$, in No. 1 fin pass top roll

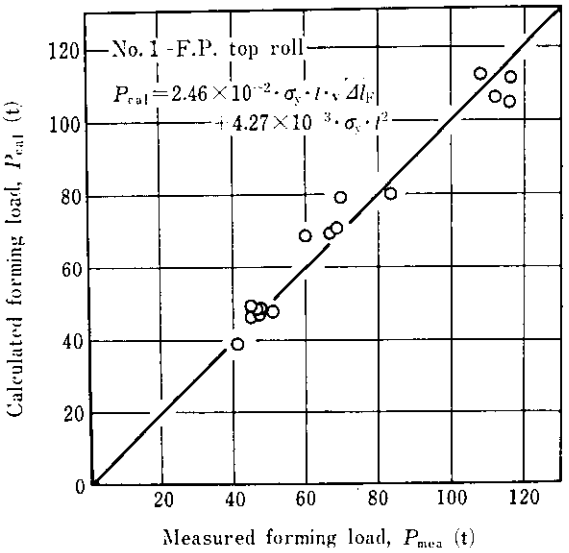

Fig. 19 Comparison between measured and calculated forming loads in No. 1 fin pass top roll

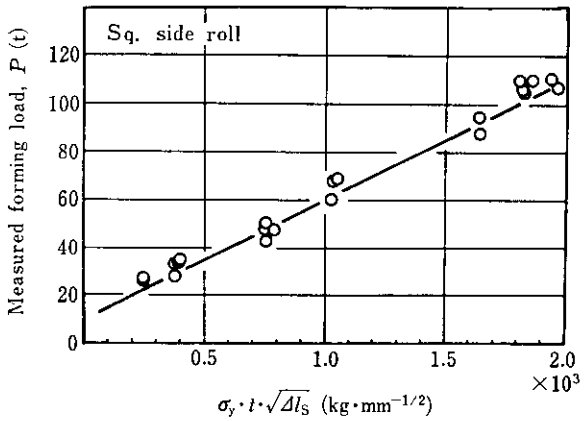

Fig. 18 Relation between forming load and a parameter, $\sigma_y \cdot t \cdot \sqrt{\Delta l_S}$, in squeeze side roll

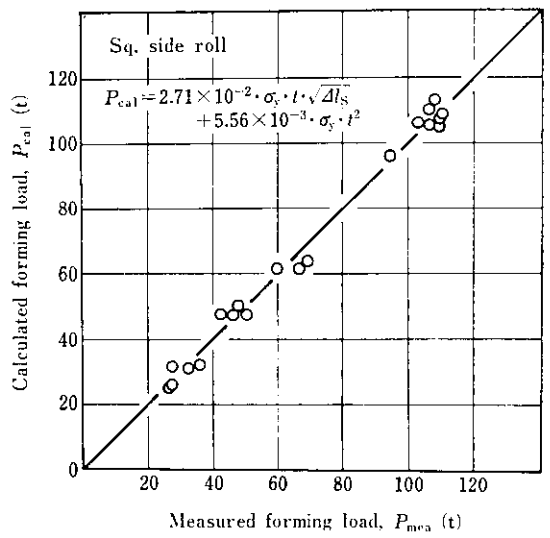

Fig. 20 Comparison between measured and calculated forming loads in squeeze side roll

the forming load and this parameter in both cases. So, each coefficient in the righthand side in the eq. **(5)** was determined by means of multiregression analysis, and the forming load, P_{cal} (t), was expressed by the following eqs. **(6)** and **(7)**, respectively.

(1) No. 1 fin pass roll

$$P_{cal} = 2.46 \times 10^{-2}\sigma_y \cdot t \cdot \sqrt{\Delta l_F} + 4.27 \times 10^{-3}\sigma_y \cdot t^2 \quad \cdots\cdots\cdots\cdots\cdots\cdots (6)$$

(2) Squeeze side roll

$$P_{cal} = 2.71 \times 10^{-2}\sigma_y \cdot t \cdot \sqrt{\Delta l_S} + 5.56 \times 10^{-3}\sigma_y \cdot t^2 \quad \cdots\cdots\cdots\cdots\cdots\cdots (7)$$

Comparison between measured and calculated forming loads shown in **Figs. 19** and **20** indicates a good correspondence between them, though with a little variation. In the actual 26 in. mill, values of R_1 and θ in the eq. **(5)** are common to each size showing $R_1 = 300$ mm, $\theta = 50°$ for No. 1 fin pass roll, and $R_1 = 300$ mm, $\theta = 70°$ for squeeze side roll.

The theoretical value of the constant term ($= 2 \sin\theta\sqrt{2R_1/\pi}$), therefore, becomes 2.12×10^{-2}, and 2.60×10^{-2}, respectively, showing a good agreement with the constant value of the first term in the right-

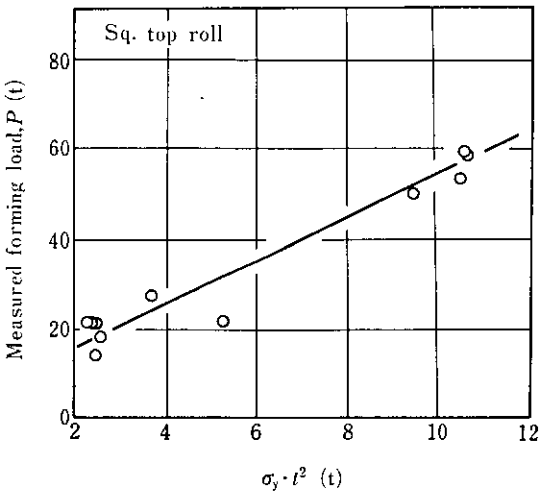

Fig. 21 Relation between forming load and a parameter, $\sigma_y \cdot t^2$, in squueze top roll

hand side of the experimental eqs. **(6)** and **(7)**. This proves that the eq. **(5)** can be considered as a fairly valid estimation equation for the forming load characteristics in fin pass roll and squeeze roll, despite the fact that in this analysis, oval approximation with 2 rolls is extended up to 4 to 5 rolls.

Fig. 21 shows that there is a linear relationship between the forming load in squeeze top roll and $\sigma_y \cdot t^2$. It is estimated that the squeeze top roll, as is apparent from its shape and usage, contributes rather to the bending forming particularly around the sheet edge than to the circumferential reduction forming such as on the squeeze side roll and fin pass roll.

5 Summary

Behavior of steel sheet deformation (as expressed in strain history, projection trace and forming flowers) and forming load at fin pass rolls and squeeze rolls have been investigated in the 26 in. cage forming ERW pipe mill. The results are as follows:

(1) For the surface strain in the forming process of 24 in. $\phi \times 6.35$ mm (X-60), a rapid tensile-compressive deformation is observed especially in the longitudinal direction of the sheet edge before and after the entrance to roll, the multitude being almost equal to the bending and unbending strain due to fitting of the sheet to roll.

(2) Different from the conventional grooved roll forming like the breakdown roll forming, a gentle and smooth transition in the surface strain is observed in the cage zone of the cage roll forming.

(3) For the longitudinal strain of the sheet edge, a gradual increase in compressive strain is observed in the cage zone, followed by a fairly large compressive and then tensile strain directly before No. 1 fin pass roll.

(4) Circumferential reduction is apparently much larger in No. 1 fin pass roll forming, while reduction in terms of circumferential strain at the center is larger in No. 2 fin pass roll forming. This can be explained by the fact that No. 1 fin pass roll forming is almost totally concentrated around the edge to contribute to the local increase in wall thickness there, while No. 2 fin pass roll forming is distributed almost uniformly in the circumferential direction.

(5) The increase in the wall thickness in the circumferential direction caused by fin pass forming shows a maximum value at about 10 mm from the edge and the constant volume equation ($\epsilon_l + \epsilon_C + \epsilon_t$) approximately stands, among the tri-axial strains.

(6) In transition in projection trace at the edge and center in the forming process, the center line (i.e. bottom line) shows a fall corresponding to downhill height (0.8 × O.D.), whereas the edge line rises up to $\Delta H_{max} \cong 0.5 \times$ O.D. in the cage zone, after which it falls gently to shift into the fin pass forming.

(7) The forming load in fin pass roll and squeeze roll can be expressed approximately in the following equation by the summation of forces which are necessary for the circumferential reduction and the bending of sheet.

$$P = 2\sigma_y \cdot t \cdot \sin\theta \cdot \sqrt{2R_1/\pi} \cdot \sqrt{\Delta l_C} + \alpha \cdot \sigma_y \cdot t^2$$

(8) Using the above theoretical equation for the forming load, the experimental formula determined by multiregression analysis was obtained as follows:

$$P_{cal} = 2.46 \times 10^{-2}\sigma_y \cdot t \cdot \sqrt{\Delta l_F} + 4.27 \times 10^{-3}\sigma_y \cdot t^2$$

and for squeeze side roll,

$$P_{cal} = 2.71 \times 10^{-2}\sigma_y \cdot t \cdot \sqrt{\Delta l_S} + 5.56 \times 10^{-3}\sigma_y \cdot t^2$$

The constant value of first term in the right-hand side of each equation showed a good agreement with the theoretical value ($= 2 \sin\theta \cdot \sqrt{2R_1/\pi}$). The authors wish to acknowledge the instructive advice on model mill cage roll forming in this research given by Dr. Onoda, Assist. Prof. Precision Engineering. Faculty of Engineering, Yamanashi University.

References

1) T. Tamura, Y. Hosokawa, et al.: *Kawasaki Steel Technical Report*, **11** (1979) 3, p. 143 (in Japanese)
2) W. Honjo, M. Nakamura et al.: *Ishikawajima-Harima Engineering Review*, **19** (1979) 1, p. 1
3) W. Honjo, M. Nakamura et al.: *Ishikawajima-Harima Engineering Review*, **19** (1979) 2, p. 67
4) H. Gondo, H. Haga et al.: *Seitetsu Kenkyu*, (1979) 297, p. 84
5) E. Yokoyama, M. Yamagata et al.: *Kawasaki Steel Technical Report*, **10** (1978) 1, p. 23 (in Japanese)
6) J. Muraki, M. Nogami et al.: *Seitetsu Kenkyu*, (1973) 277, p. 25
7) S. Kikushima, U. Nakamura et al.: *Ishikawajima-Harima Engineering Review*, **18** (1978) 5, p. 405
8) Y. Onoda, J. Kokade et al.: *Journal of the Japan Society for Technology of Plasticity*, **20** (1979) 222, p. 601
9) H. Suzuki, M. Kiuchi et al.: *Journal of the Japan Society for Technology of Plasticity*, **18** (1977) 196, p. 365
10) H. Suzuki, M. Kiuchi et al.: *Journal of the Japan Society for Technology of Plasticity*, **11** (1970) 112, p. 315
11) Y. Saito, Y. Fujita et al.: *Journal of the Japan Society for Technology of Plasticity*, **13** (1972) 143, p. 907
12) K. Nakajima, W. Mizutani et al.: *Tetsu-to-Hagané*, **59** (1973) 9, A125
13) K. Nakajima, W. Mizutani et al.: *Seitetsu Kenkyu*, (1979) 299, p. 108
14) E. Ikushima, Y. Mihara et al.: *Tetsu-to-Hagané*, **64** (1978) 4, S269
15) Z. Baba: *Sumitomo Metals*, **15** (1963) 2, p. 19
16) H. Ikutame: *Journal of the Japan Society for Technology of Plasticity*, **8** (1967) 82, p. 591
17) Y. Azuma, N. Torii et al.: *The 57th Symposium of J.S.T.P.*, (1976), p. 64
18) H. Gross: *Herstellung von Rohren, Verein Deutscher Eisenhüttenleute, Verlag stahleisen M.B.H.* Dusserdorf, (1975) p. 80
19) D. Anderson and P. Mackinnon: *Technical Report of the Steel Company of Canada*, (1973) p. 204
20) H. Nakajima, W. Mizutani et al.: *The Proceedings of the* 1976 *Japanese Spring Conference for the Technology of Plasticity*, (1976) p. 285
21) M. Kiuchi, K. Shintani et al.: *The Proceedings of the* 1980 *Japanese Spring Conference for the Technology of Plasticity*, (1980) p. 287
22) Y. Onoda, Y. Uematsu et al.: *The 31th Japanese National Conference for the Technology of Plasticity*, (1980) p. 234
23) Y. Onoda, Y. Uematsu et al.: *The 31th Japanese National Conference for the Technology of Plasticity*, (1980) p. 235
24) H. Nakajima, W. Mizutani et al.: *The 23th Japanese National Conference for the Technology of Plasticity*, (1972) p. 455
25) H. Nakajima, W. Mizutani et al.: *The Proceedings of the* 1976 *Japanese Spring Conference for the Technology of Plasticity* (1976) p. 281
26) M. Masuda, T. Murota et al.: *Journal of the Japan Society for Technology of Plasticity*, **6** (1965) 54, p. 379
27) H. Suzuki, M. Kiuchi et al.: *Journal of the Japan Society for Technology of Plasticity*, **11** (1970) 119, p. 913
28) H. Nakajima, W. Mizutani et al.: *The 26th Japanese National Conference for the Technology of Plasticity*, (1975) p. 11
29) H. Nakajima, W. Mizutani et al.: *The Proceedings of the* 1976 *Japanese Spring Conference for the Technology of Plasticity*, (1976) p. 289